Optica Applicata, Vol. XXVII, No. 4, 1997

Studies of homogeneous fibres using speckle photography

A. M. HAMED, H. EL-GHANDOOR

Physics Department, Faculty of Science, Ain Shams University, Cairo, Egypt.

The imaging intensity distribution of light passing through a phase object in the form of an array of homogeneous fibres located on a ground glass of constant refractive index μ_d is presented. The speckle pattern formed is recorded twice on the same film, where the first exposure is taken with the ground glass alone, while the second exposure is taken with the fibres stacked on the ground glass. After processing the specklegram formed, when illuminated by a laser beam, displays a $\cos^2$ function modulated by the fibre functional distribution. The optical path difference between light propagating through the ground glass alone and light passing through the fibre and the ground glass is calculated. The three dimensional representation of the optical thickness variation of the fibre has been extracted from the resulting interference pattern.

1. Introduction

It has been reported [1]–[7] that a coherently illuminated translated diffuser produces dynamic speckles which reveal two kinds of movement, *i.e.*, lateral translation of a whole pattern as a rigid body and structural change of each speckle element. A double exposure speckle technique for imaging system analysis [8] has been reported and is experimentally verified. This technique is based on decorrelation of speckle patterns, which occurs as the laser-illuminated diffuser is translated laterally in its plane. A specklegram, exposed before and after diffuser translation, contains a large number of path pairs whose degree of correlation can be related to the imaging quality of the optical system through which the speckle patterns are produced.

In this study, a feasible method is presented allowing us to extract the optical thickness variation of a homogeneous fibre using modulation. The problem is theoretically analyzed in Sect. 2, obtaining the intensity distribution of the scattered light in the presence of the phase object. In Sect. 3, the optical path difference is calculated followed by experimental results. A three-dimensional representation of the optical thickness variation of the homogeneous fibre is presented. Finally, a discussion of the results and a conclusion are given.

2. Theoretical analysis

Assume that $d(x,y)$ is a randomly distributed function representing the complex amplitude of the diffuser (ground glass). Let $g(x,y)$ be a phase object composed of

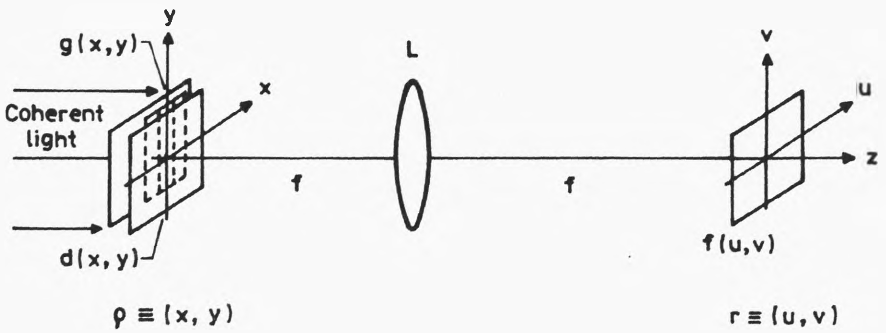

Fig. 1. Coding set-up of the composite transparency. $f(x,y) = g(x,y)d(x,y)$, where $g(x,y)$ – array of cylindrical fibres of homogeneous refractive index situated in the plane (x,y), $d(x,y)$ – randomly distributed function of the ground glass, $\rho \equiv (x,y)$ – radial coordinate in the object plane, $r \equiv (u,v)$ – radial coordinate in the Fourier plane

an array of cylindrical fibres of homogeneous medium and uniform circular cross-section as shown in Fig. 1. Then, the complex amplitude transmittance is represented as follows:

$$f(x,y) = d(x,y)g(x,y) \tag{1}$$

where $g(x,y)$ is written in polar coordinates as

$$g(\rho;z) = \mathrm{cyl}(\rho;z) * \sum_{n=0}^{N} \delta(\rho - nd_f) \tag{2}$$

where $g(\rho)$ is rewritten at a constant value of z as

$$g(\rho) = \mathrm{circ}(\rho) * \sum_{n=0}^{N} \delta(\rho - nd_f), \tag{2a}$$

N – number of fibres arranged in the array,
$d_f = 2r_f$ – cross-sectional diameter of each fibre,
δ – Dirac delta distribution,
ρ – radial coordinate of the fibre cross-section corresponding to the Cartesian coordinates (x,y).

Equation (2a) can be rewritten as follows:

$$g(\rho) = \sum_{n=0}^{N} \mathrm{circ}(\rho - nd_f). \tag{3}$$

The complex amplitude of the modulated speckle pattern recorded at a sufficiently great distance is computed by operating the Fourier transform upon Eq. (1) as follows:

$$\tilde{f}(u,v) = \mathrm{F.T.}[d(x,y)g(x,y)]. \tag{4}$$

$\tilde{f}(u,v)$ is the complex amplitude of the modulated speckle pattern recorded in the

Fourier plane (u, v). Now, making use of the properties of convolution theorem, Eq. (4) becomes

$$\tilde{f}(u,v) = \text{F.T.}[d(x,y)] * \text{F.T.}[g(x,y)] = \tilde{d}(u,v) * \tilde{g}(u,v) \tag{5}$$

where

$$\tilde{d}(u,v) = \iint\limits_{-\infty}^{\infty} d(x,y)\exp\left[-\frac{2\pi j}{\lambda f}(ux+vy)\right]dx\,dy, \tag{6}$$

$\tilde{d}(u,v)$ is the complex amplitude of the ordinary speckle pattern obtained in the absence of any modulation, $\tilde{g}(u,v)$ is obtained by operating the Fourier transform upon Eq. (3), *i.e.*,

$$\tilde{g}(u,v) = \text{F.T.}[g(x,y)] = \text{F.T.}\left\{\sum_{n=0}^{N}\text{circ}(\rho - nd_f)\right\} = [J_1(w)/w]\sum_{n=0}^{N}\exp(jknrd_f/f) \tag{7}$$

where: $w = k\rho r/f$, f — distance between the fibre plane and the Fourier plane, $k = 2\pi/\lambda$ — propagation constant, r — radial coordinate corresponding to the Cartesian coordinates (u, v) situated in the Fourier plane.

Substituting from Eq. (6) and (7) into Eq. (5), we finally get this result:

$$\tilde{f}(u,v) = \tilde{d}(u,v) * \frac{J_1(w)}{w}\sum_{n=0}^{N} exp(jknrd_f/f). \tag{8}$$

Referring to Eq. (8), it is clear that the resulting speckle pattern is equal to the ordinary speckle pattern convoluted with the distribution of the Airy patterns multiplied by a sum of complex functions representing the location of each fibre.

Suppose that two successive exposures are taken with equal symmetric displacements, where the first exposure is taken with the ground glass alone and the second exposure is taken in the presence of fibres stacked on the ground glass. Hence the complex amplitudes of the recorded speckles in each case are written as follows:

$$\tilde{f}_1(\bar{r}) = \tilde{d}(\bar{r}) * \delta(\bar{r} - \bar{r}_0), \tag{9}$$

$$\tilde{f}_2(\bar{r}) = \tilde{d}(\bar{r}) * \delta(r + r_0) * \sum_{n=0}^{N}\frac{2J_1(w)}{w}\exp(jkrnd_f/f) \tag{10}$$

where r_0 is the amount of the lateral shift occurring between the two exposures. Taking into consideration that the shift r_0 is greater than the average grain size of speckles, hence the total recorded intensity becomes

$$I_T(\bar{r}) = |\tilde{f}_1(\bar{r})|^2 + |\tilde{f}_2(\bar{r})|^2. \tag{11}$$

Processing the high resolution photographic plate under linear conditions, the transmitted amplitude becomes nearly proportional to the recorded intensity, *i.e.*,

$$t(\bar{r}) \simeq |\tilde{f}_1(\bar{r})|^2 + |\tilde{f}_2(\bar{r})|^2. \tag{12}$$

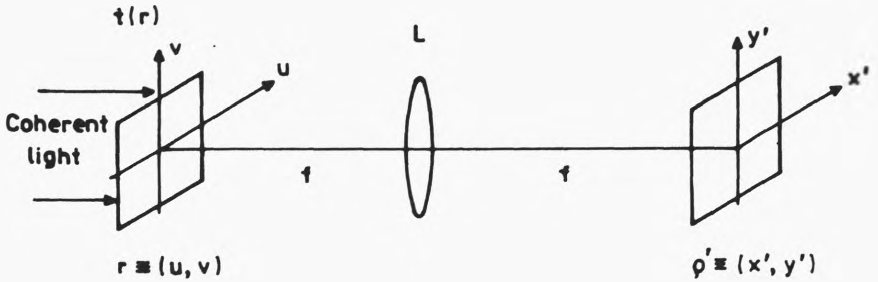

Fig. 2. Reconstruction process of the modulated pattern: $t(r) \simeq I_T(r)$, L — achromatic converging lens

The processed plate is illuminated with a spatially coherent beam emitted from He-Ne laser at $\lambda = 6328$ Å using a well corrected converging lens, as shown in Fig. 2. The complex amplitude obtained in the Fourier plane of the imaging lens is computed as

$$A(\rho') = \text{F.T.}[t(\bar{r})] = \text{F.T.}\{|\tilde{f}_1(\bar{r})|^2 + |\tilde{f}_2(\bar{r})|^2\} \tag{13}$$

where $\rho' = (x', y')$ is the radial coordinate in the imaging plane of the imaging system.

Operating this transformation and making use of the properties of convolution theorem, we can write $A(\rho')$ as

$$A(\rho') = f_1(\rho') * f_1^*(\rho') + f_2(\rho') * f^*(\rho') \tag{14}$$

where

$$f_{1,2}(\rho') * f_{1,2}^*(\rho') = \text{F.T.}|\tilde{f}_{1,2}(\bar{r})|^2.$$

Substituting from Eq. (9) and Eq. (10) into Eq. (14), we get this result to represent the complex amplitude formed in the imaging plane

$$A(\rho') = [d(\rho')\exp(jkr_0\rho'/f) * d^*(\rho')\exp(-jkr_0\rho'/f)]$$
$$+ \left[d(\rho')\exp(-jkr_0(\rho')/f) \sum_{n=0}^{N} \text{circ}(\rho' - nd_f) * d^*(\rho')\exp(jkr_0\rho'/f) \sum_{n=0}^{N} \text{circ}(\rho' - nd_f) \right], \tag{15}$$

* — complex conjugate.

Consequently, the recorded intensity in the imaging plane $\rho' = (x', y')$ is computed as follows:

$$I(\rho') = |C_1(\rho') + C_2(\rho')|^2 = |C_1(\rho')|^2 + |C_2(\rho')|^2 + C_1(\rho')C_2^*(\rho') + C_1^*(\rho')C_2(\rho') \tag{16}$$

where:

$$C_1(\rho') = d(\rho')\exp(jkr_0\rho'/f) * d^*(\rho')\exp(-jkr_0\rho'/f),$$

$$C_2(\rho') = d(\rho')\exp(-jkr_0\rho'/f) \sum_{n=0}^{N} \text{circ}(\rho' - nd_f) * d^*(\rho')\exp(jkr_0\rho'/f) \sum_{n=0}^{N} \text{circ}(\rho' - nd_f).$$

Considering that the image of the fibres is slightly varied inside the second autocorrelation function $C_2(\rho')$, then we can write $C_2(\rho')$ as follows:

$$C_2(\rho') = C_1(\rho') \sum_{n=0}^{N} \mathrm{circ}(\rho' - nd_f). \tag{17}$$

Omitting the term $|C_1|^2$ in order to improve the S/N ratio of the image described by Eq. (16), the obtained image becomes

$$I(\rho') = G(\rho')\cos^2(kr_0\rho'/f)[d(\rho') * d^*(\rho')] \tag{18}$$

where $G(\rho')$ is the geometrical image of the object described in Eq. (4).

It is clear that the obtained image of the fibres is modulated by $\cos^2$ function considering that the autocorrelation function $d(\rho') * d^*(\rho')$ is a background noise. In the following section, we compute the optical path difference of the light propagating through the object.

3. Calculation of the optical path difference

The optical path of light propagating along the diffuser alone and that passing through the fibre and diffuser are computed. The optical path difference (O.P.D.) between these two paths is obtained. Referring to the geometry of Fig. 3, the optical

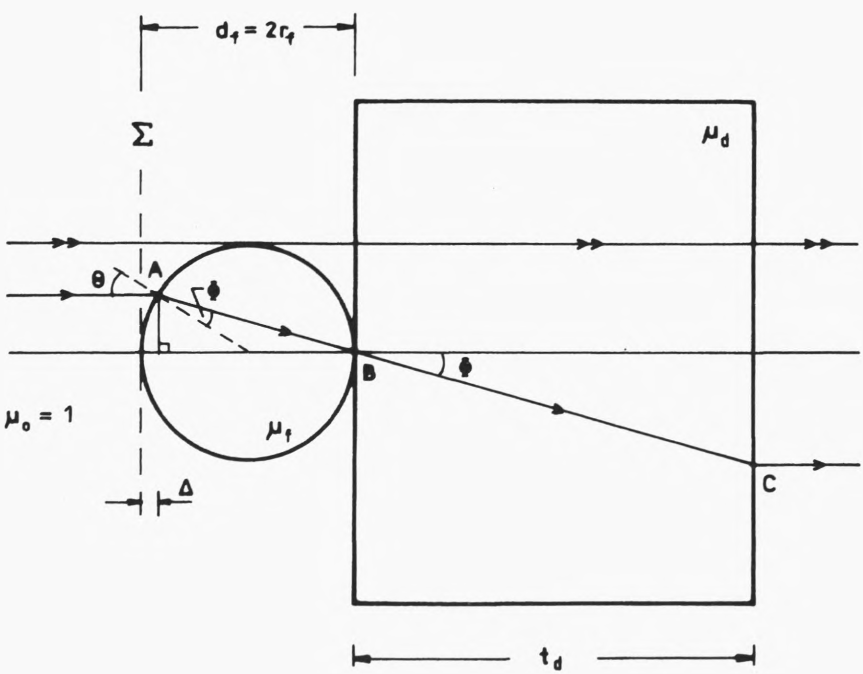

Fig. 3. Optical path trajectory inside one fibre of refractive index μ_f compared with the path trajectory in the ground glass only. μ_d — refractive index of the ground glass, t_d — thickness of ground glass, r_f — fibre radius, Σ — wavefront

path of light propagating through the diffuser is

$$x_1 = 2r_f + \mu_d t_d \tag{19}$$

where: μ_d – refractive index of the ground glass, t_d – thickness of the ground glass, $d_f = 2r_f$ – fibre diameter. The optical path of light propagating through the fibre and diffuser is

$$x_2 = \Delta_1 + AB\mu_f + BC\mu_d \tag{20}$$

where: μ_f – refractive index of the fibre,

$$\begin{aligned} \Delta_1 &= 2r_f \sin^2\Phi, \\ AB &= 2r_f \cos\Phi, \\ BC &= t_d \sec\Phi. \end{aligned} \tag{21}$$

Substituting from Eq. (21) into Eq. (20), we get x_2 as

$$x_2 = 2r_f \sin^2\Phi + 2\mu_f r_f \cos\Phi + \mu_d t_d \sec\Phi \tag{22}$$

where Φ is the angle of refraction inside the fibre. Hence, O.P.D. = $x_2 - x_1$ is obtained as

$$\text{O.P.D.} = \mu_d t_d[\sec\Phi - 1] + 2r_f[\sin^2\Phi + \mu_f \cos\Phi - 1]. \tag{23}$$

Using Snell's law for refraction, we finally get this result

$$\text{O.P.D.} = \mu_d t_d\left[\frac{\mu_f}{\sqrt{\mu_f^2 - \sin^2\theta}} - 1\right] + 2r_f\left[\mu_f^2 - \sin^2\theta)^{1/2} + \frac{\sin^2\theta}{\mu_f^2} - 1\right]. \tag{24}$$

It is clear that the O.P.D. is dependent upon the angle of incidence θ for certain parameters of μ_d, μ_f, t_d and d_f, *i.e.*,

$$\text{O.P.D.} = f(\theta; \mu_f, \mu_d, t_d, d_f).$$

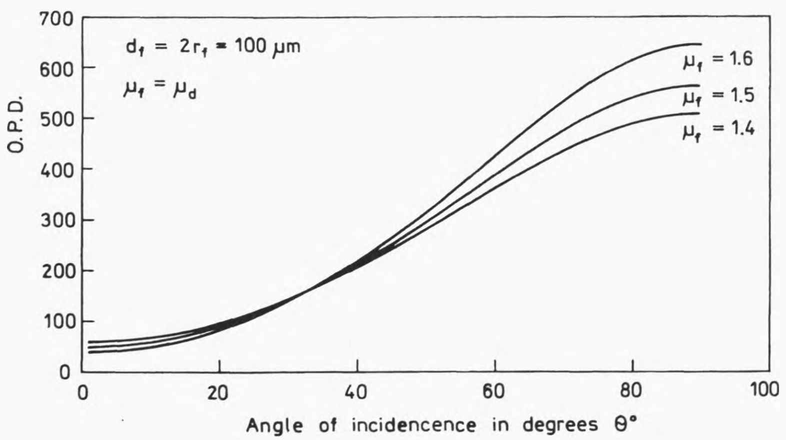

Fig. 4. Variation of the optical path difference with the angle of incidence (in degrees) using a fibre placed on a ground glass as a diffuser

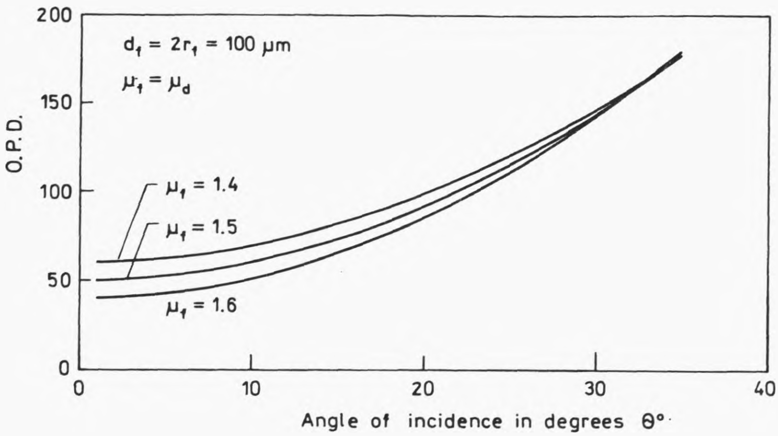

Fig. 5. Variation of the optical path difference with the angle of incidence (in degrees) in the range from 0° to 35°

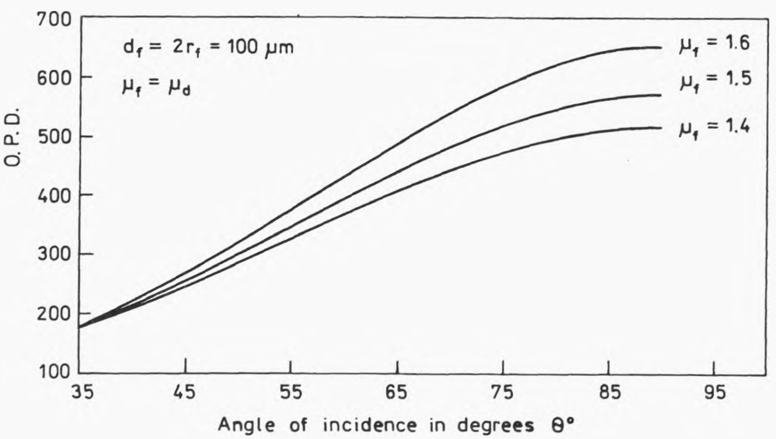

Fig. 6. Variation of the optical path difference with the angle of incidence (in degrees) in the range from 35° to 90°

The optical path difference vs. the angle of incidence θ is computed using Eq. (24) for different angles ranging from 0 to $\pi/2$ as shown in Fig. 4. From the results obtained, it is clear that the O.P.D. is greater for $\mu_f = 1.4$ than for $\mu_f = 1.5$ and $\mu_f = 1.6$ in the range $0° - 35°$, as shown in Fig. 5, while it becomes smaller for higher values of angles of incidence situated in the range $35° - 90°$, as shown in Fig. 6.

4. Experimental results

The optical arrangement is described as in Fig. 1. A collimated beam of He-Ne laser is allowed to be incident on the ground glass containing the fibre bundle. Two successive exposures are taken on a high resolution photographic plate, making

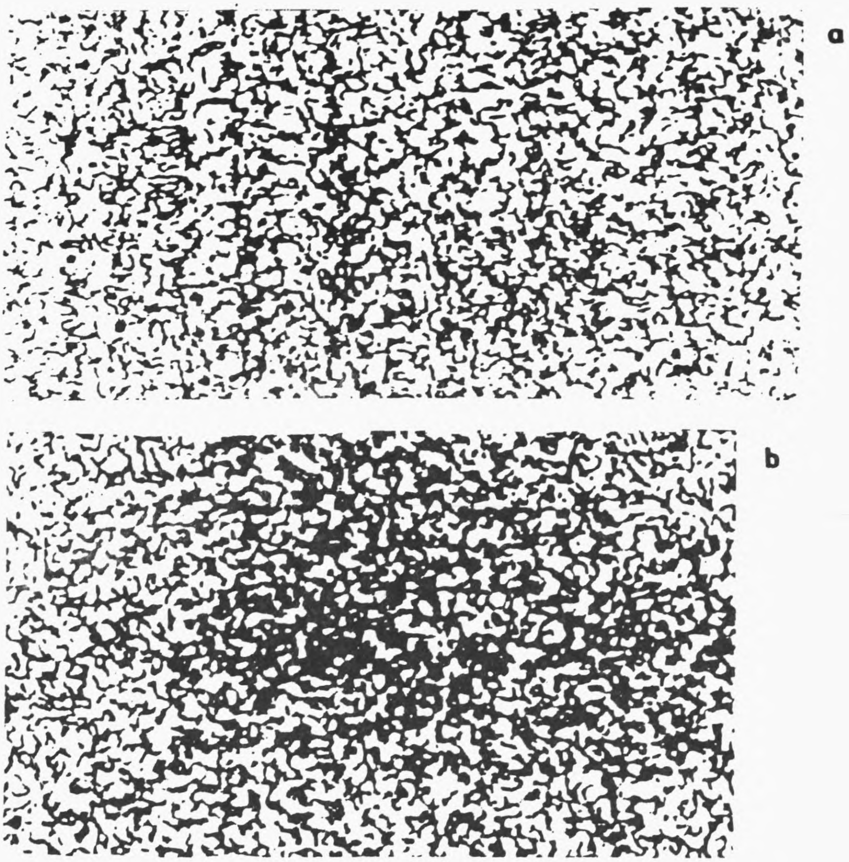

Fig. 7. Speckles modulated by a bundle of fibres as a phase object (**a**). Ordinary speckle pattern (**b**)

a lateral displacement of nearly 60 μm between exposures. The first exposure is taken with the ground glass alone while the second exposure is taken with the fibres stacked on the ground glass. Due to light deflection through the fibre region two identical speckle patterns are recorded changing their shift and orientation. The modulated speckle pattern is recorded as shown in Fig. 7**a**, and compared with that obtained in the absence of the fibres as a phase object in Fig. 7**b**.

After processing the photographic plate under linear conditions using the reconstruction system shown in Fig. 2, the obtained fringes localized in the focal plane of the transforming lens shown in Fig. 8 are fed to a CCD camera, which enables us to measure the fringe spacing s using a personal computer. The speckle shift Δ has been calculated from the known relation $\Delta = \lambda z/s$, where z is the distance between the processed film and the screen. The obtained values of shift are fed to the computer to get a three-dimensional representation of the optical thickness variations $\mu_f t_f(r)$ of the fibre at each point r across its radius as shown in Fig. 9. t_f is varied along the fibre cross-section, while μ_f has a constant value. As the fibre is an

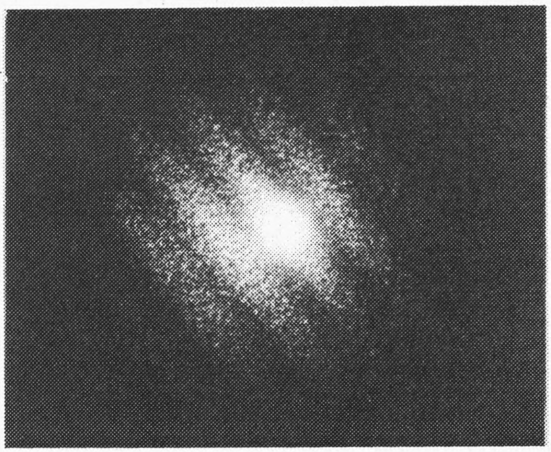

Fig. 8. Photograph of the fringes obtained in the focal plane of the Fourier transforming lens using the optical system shown in Fig. 2

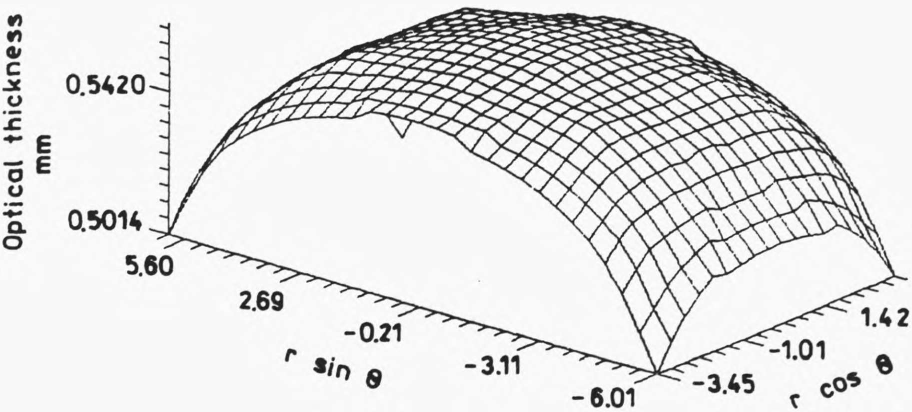

Fig. 9. Reconstruction of fiber optical thickness profile with 14 projections

axisymmetric phase object, the recording of its optical thickness can be considered the same along different directions (projections). The data obtained along one direction of the fibre thickness and refractive index are the same along 14 projections or illumination direction. These data are used to get a three-dimensional profile of the fibre optical thickness.

5. Discussion and conclusions

The optical path trajectory of light passing through fibres of circular cross-section located on a ground glass is obtained. It is shown from the results obtained that the light trajectory resembles an inverted truncated Gaussian distribution. Referring to Fig. 4, it is clear that the optical path difference has a minimum value along the optical axis when the angle of incidence is very small, while the optical path is longer for greater angles of incidence. It is concluded that the theoretical analysis is in good agreement with the obtained fringes localized in the focal plane of the imaging lens. The reconstructed fibre profile is extracted from the obtained experimental data.

Acknowledgment — We are grateful to Prof. N. Barakat for reading the manuscript.

References

[1] Yamaguchi I., Komatsu S., Saito H., Jpn. J. Appl. Phys., Suppl., **14** (1975), 301.
[2] Courjon B., Reggiani M., Bulabois J., Jpn. J. Appl. Phys., Suppl., **14** (1975), 311.
[3] Barakat N., Hamed A. M., El-Ghandoor H., Abd El Ghaffar O. A., J. Modern Opt. **38** (1991), 203.
[4] Barker D. R., Fourney M. E., Opt. Lett. **1** (1977), 136.
[5] Barakat N., Hamed A. M., El-Ghandoor, Optik **78** (1987), 102.
[6] Erf R. K., *Speckle Metrology*, Academic Press, New York 1978.
[7] Kopf U., Opt. Commun. **5** (1972), 347.
[8] Komatsu S., Sumi K., Ohzu H., Appl. Opt. **28** (1989), 1869.

Received May 22, 1997
in revised form October 20, 1997